Promoting Ag/Al2O3 Performance in Low-Temperature H2-C3H6-SCR by Thermal Pretreatment of γ-Alumina in Water

Tesnim Chaieb, Laurent Delannoy, Catherine Louis, Cyril Thomas

Promoting Ag/Al_2O_3 performance in low-temperature H_2-C_3H_6-SCR by thermal pretreatment of γ-alumina in water

Tesnim Chaieb, Laurent Delannoy, Catherine Louis and Cyril Thomas*

1- Sorbonne Universités, UPMC Univ Paris 06, UMR CNRS 7197, Laboratoire de Réactivité de Surface, 4 Place Jussieu, Tour 43-53, 3ème étage, Case 178, F-75252, Paris, France

Running title: Promoting Ag/Al_2O_3 performance in H_2-C_3H_6-SCR

* To whom correspondence should be addressed:

Dr. Cyril Thomas

Sorbonne Universités, UPMC Univ Paris 06, UMR CNRS 7197, Laboratoire de Réactivité de Surface, 4 Place Jussieu, Tour 43-53, 3ème étage, Case 178, F-75252, Paris, France

e-mail: cyril.thomas@upmc.fr

Tel: + 33 1 44 27 36 30

Fax: + 33 1 44 27 60 33

Abstract:

The present work highlights for the first time that a thermal treatment of γ-Al_2O_3 in water at 80 °C for 24 h prior to Ag deposition (Ag/Al_2O_3-OH) leads to a drastic enhancement of H_2-C_3H_6-SCR performance at low temperature. This enhancement is attributed to the higher NO_x coverage on Ag/Al_2O_3-OH compared with that of Ag/Al_2O_3. The higher NO_x adsorption capacity of the sample prepared from the γ-Al_2O_3 thermally-treated in water is proposed to result from the preferential interaction of Ag with newly-created Al_2O_3 anchoring sites ($Al(OH)_3$ bayerite domains), which were not available on the untreated pristine support.

Key Words: Selective Catalytic Reduction; NO_x-TPD; UV-vis

1. Introduction

Since the implementation of catalytic converters dedicated to the concomitant reduction of nitrogen oxides (NO_x = NO + NO_2) and oxidations of carbon monoxide (CO) and unburned hydrocarbons (HCs) in the early 1970s, the environmental challenge has moved to the reduction of NO_x from lean exhausts at low temperatures [1]. Even though the Selective Catalytic Reduction of NO_x by ammonia (NH_3-SCR) and Lean-NO_x Traps (LNT) remain as the only technologies to comply with the current emission standards, these two technologies exhibit drawbacks [1,2] and many studies have been devoted to seek out for alternative processes such as the reduction of NO_x by hydrocarbons (Hydrocarbon Selective Catalytic Reduction: HC-SCR).

In 1993, Miyadera firstly brought to the attention of the community that Ag/Al_2O_3 could be a promising catalyst in HC-SCR with various light hydrocarbons [3]. Few years later, Satokawa and co-workers discovered that the performance of the Ag/Al_2O_3 catalyst could be improved drastically at low temperatures (below 300 °C) on the addition of small quantities of H_2 in the reacting feed (H_2-HC-SCR) [4,5]. The Ag/Al_2O_3 system has been investigated thoroughly until recently [6-8].

Since these pioneering works, no major improvement of the Ag/Al_2O_3 system has been achieved up to the works of Kamolphop et al. [9] and Petitto and Delahay [10] in which superior HC-SCR performance was obtained using long-chain alkanes as reductants and catalysts prepared by ball-milling compared with those synthesized by the conventional impregnation techniques reported to date. Ball-milled prepared Ag/Al_2O_3 catalysts were also found to exhibit higher H_2-HC-SCR activities in comparison with the conventionally prepared samples [11,12]. This was inferred to modifications of the catalyst surface and more specifically to changes in the affinity of the Al_2O_3 surface towards water and decane [11]. In addition, it was found that isocyanates (–NCO), which are supposed to be key intermediates

of HC-SCR reactions [1], were formed quicker and had a higher surface concentration on the ball-milled catalyst compared with the conventionally prepared sample [11,12].

Since it has been proposed that Ag anchored onto the Al_2O_3 support via the interaction with its hydroxyl groups (Al-OH + Ag^+ = Al-O-Ag + H^+) during the impregnation step [13] and that hydroxylation of Al_2O_3 occurs when immersed into water under various experimental conditions (temperature, pressure, pH, time of exposure) [14-16], we found of particular interest to investigate the influence of the hydroxylation of γ-Al_2O_3 prior to Ag deposition on C_3H_6- and H_2-C_3H_6-SCR catalytic performance. To our knowledge, such an approach has never been reported previously for the Ag/Al_2O_3 system, but recently in the case of the Pt/Al_2O_3 system for other catalytic reactions [17].

2. Experimental

2.1. Catalyst synthesis

Hydroxylation of the γ-Al_2O_3 support (Procatalyse, 180 m^2/g) was carried out by heating this oxide in distilled water at 80 °C for 24 h under vigorous stirring. After filtering, the solid was dried and kept under vacuum at RT. Ag was deposited following the incipient wetness procedure described in our earlier works [6,8]. Briefly, Ag was deposited via incipient wetness impregnation of an aqueous solution $AgNO_3$ (Aldrich, >99%) on the hydroxylated Al_2O_3 sample (0.7 cm^3/g porous volume) to achieve a silver loading of 1.9 wt%, which was ascertained by inductively coupled plasma atomic emission spectroscopy (ICP-AES, Centre d'Analyse du CNRS, Solaize, France). In parallel, a new batch of Ag/Al_2O_3 sample was prepared from the as-received Al_2O_3 support following the abovementioned Ag deposition procedure. From here on, the samples prepared from hydroxylated Al_2O_3 will be denoted as Al_2O_3-OH and Ag/Al_2O_3-OH and compared with the samples synthesized from the

untreated support denoted as Al_2O_3 and Ag/Al_2O_3 (1.8 wt% Ag) either newly-prepared or studied earlier [6,8].

2.2. C_3H_6-SCR and H_2-C_3H_6-SCR runs

The steady state catalytic C_3H_6-SCR and H_2-C_3H_6-SCR experiments were carried out in a U-type quartz reactor (12 mm i.d.). The temperature of the tubular furnace was set by a Eurotherm 2408 temperature controller using a K type thermocouple. Prior to the SCR experiments, the samples (0.18 g of Ag/Al_2O_3 or Ag/Al_2O_3-OH diluted in 0.18 g of Al_2O_3, 125-200 µm) were calcined in situ in O_2 (20 %)-He at 550 °C (3 °C/min) for 2 h with a flow rate of 100 mL_{NTP}/min. After cooling to 150 °C, the samples were submitted to a C_3H_6-SCR experiment from 150 to 550 °C [6]. The samples were subsequently exposed to the H_2-C_3H_6-SCR feed at 150 °C. H_2 (2 %/He), NO (4000 ppm/He), C_3H_6 (2000 ppm/He), O_2 (100 %) and He (100 %) were fed from independent cylinders (Air Liquide) without any further purification via mass flow controllers (Brooks 5850TR). Typically, the composition of the SCR feeds was: 0 or 0.21 % H_2, 385 ppm NO_x (~ 96 % NO), 400 ppm C_3H_6 and 8 % O_2 in He, and the total flow rate was 230 mL_{NTP}/min. In both SCR experiments, the temperature was increased stepwise from 150 to 550 °C with 25 °C increments and left for about 1 h at each temperature step. Steady state activity was found to be achieved shortly for all reaction temperatures. The reactor outflow was analyzed using a µ-GC (Agilent Technologies, CP4900) equipped with two channels. The first channel, a 5A molecular sieve column (80 °C, 150 kPa He, 200 ms injection time, 30 s backflush time), was used to separate N_2, O_2 and CO. The second channel, equipped with a poraplot Q column (60 °C, 150 kPa He, 200 ms injection time), was used to separate CO_2, N_2O, C_3H_6 and H_2O. A chemiluminescence NO_x analyzer (Thermo Environmental Instruments 42C-HT) allowed the simultaneous detection of both NO and NO_2. NO_x conversion to N_2 and N_2 selectivity were calculated as follows:

$$X_{NOx\ to\ N2}\ (\%) = (2 \times [N_2])/[NO_x]_{inlet}\ ) \times 100 \qquad \text{(Eq. 1)}$$

$$S_{N2}\ (\%) = ([N_2]/[N_2+N_2O]) \times 100 \qquad \text{(Eq. 2)}$$

where $[NO_x]_{inlet}$, $[N_2]$ and $[N_2O]$ were the concentrations in NO_x measured at the inlet of the reactor and in N_2 and N_2O at the outlet of the reactor. C_3H_6 conversions were calculated on the basis of the CO_x (CO + CO_2) products formed:

$$X_{C3H6}\ (\%) = (([CO] + [CO_2])/([C_3H_6]_{inlet} \times 3)) \times 100 \qquad \text{(Eq. 3)}$$

where [CO], $[CO_2]$ and $[C_3H_6]_{inlet}$ were the concentrations of CO and CO_2 measured at the outlet of the reactor and that of C_3H_6 measured at the inlet of the reactor, respectively.

2.3. Catalyst characterization

N_2-sorption measurements were carried out on a Belsorp max instrument (Bel Japan) at 77 K. It was found that the BET surface of the hydroxylated samples both after drying at 120 °C for 12 h in an oven and calcination at 550 °C for 2 h in a muffle furnace (185 m^2/g) did not vary to a significant extent from that of the starting Al_2O_3 support (180 m^2/g).

XRD measurements were carried out from 10 to 80° by step of 0.01°using a theta-theta D8 Advance (Bruker) powder diffractometer with Cu-Kα radiation (0.154 nm) operated at 30 kV and 30 mA, and equipped with a 1D LynxEye detector set to a 3° opening.

The ultraviolet–visible diffuse reflectance spectra (UV–vis DRS) of Ag/Al_2O_3 and Ag/Al_2O_3-OH were collected on a spectrophotometer (Cary 5000, Varian) equipped with a diffuse reflectance cell at RT in ambient air from 200 to 600 nm after calcination at 550 °C for 2 h and using the corresponding calcined Al_2O_3 supports for the background spectra.

The hydroxylated materials were also characterized by the NO_x-Temperature-Programmed Desorption (NO_x-TPD) method [6,18,19]. Prior to the NO_x-TPD experiments, the samples were calcined in situ under a flow rate of 100 mL_{NTP}/min of 20% O_2 in He at 500 °C (3 °C/min) for 2 h. The samples (about 0.2 g) were firstly contacted with a NO–O_2–He

(385 ppm–8%–balance, 230 mL_{NTP}/min) mixture at room temperature (RT) until recovery of the inlet NO_x concentration. The samples were then flushed with O_2(8%)–He at RT to remove weakly adsorbed NO_x species until the disappearance of the NO_x species in the stream. The NO_x-TPD experiments were carried out from RT to 550 °C at a heating rate of 3 °C/min under a flow of 230 mL_{NTP}/min of 8% O_2 in He. The reactor outflow was continuously monitored using a chemiluminescence NO_x analyzer (Thermo Environmental Instruments 42C-HT) which allowed for the simultaneous detection of both NO and NO_2.

3. Results

3.1. SCR performance

In the absence of H_2 in the reacting feed (C_3H_6-SCR, Fig. 1), hydroxylation of Al_2O_3 prior to the addition of Ag was found to have little influence on the conversion of NO_x to N_2 (Fig. 1a, black line) although the N_2 selectivity was found to be lowered to a significant extent below 450 °C on the hydroxylated catalyst. Regarding C_3H_6 oxidation (Fig. 1b), it can be seen that the conversion profile of Ag/Al_2O_3 was steeper than that observed on Ag/Al_2O_3-OH.

As expected from the pioneering work of Satokawa [4], the conversions of NO_x to N_2 and C_3H_6 to CO_x occurred at much lower temperatures in the presence of H_2 on both samples (Fig. 2) in comparison with the reaction ran in the absence of H_2 (Fig. 1). The C_3H_6 and H_2 oxidation profiles were found to be shifted to slightly higher temperature on Ag/Al_2O_3-OH compared to Ag/Al_2O_3 (Fig. 2b). Much more interesting are the results obtained regarding the reduction of NO_x to N_2 (Fig. 2a). From 250 to 450 °C, the catalyst prepared from the support thermally-treated in water (Ag/Al_2O_3-OH) remarkably outperformed Ag/Al_2O_3 that had been prepared conventionally, whereas N_2 selectivity remained comparable on both samples (Fig. 2a). The conversion of NO_x to N_2 reached 82 %

at 275 °C on Ag/Al_2O_3-OH, whereas Ag/Al_2O_3 exhibited only 50 % conversion at the same temperature.

One can note that the newly-prepared Ag/Al_2O_3 sample showed reproducible C_3H_6-SCR and H_2-C_3H_6-SCR performance compared to the sample studied earlier (Figs. 1 and 2). Another Ag/Al_2O_3-OH sample was prepared under different pH conditions and its SCR and H_2-SCR catalytic performance (not shown) was found to be close to that reported in Figs. 1 and 2. Considering all the above, the present results highlights for the first time on the beneficial effect of a thermal pretreatment of the pristine γ-Al_2O_3 support in water prior to Ag deposition on H_2-C_3H_6-SCR performance. To gain further insights into the enhanced H_2-C_3H_6-SCR performance of the Ag catalyst prepared from the γ-Al_2O_3 support thermally-pretreated in water compared with that prepared from the as-received Al_2O_3, the samples were characterized by XRD, UV-visible spectroscopy and NO_x-TPD.

3.2. Catalyst characterization

XRD characterization of Al_2O_3, Al_2O_3-OH and calcined Ag/Al_2O_3-OH is shown in Fig. 3. Narrow diffraction peaks appeared at 18.6, 20.3, 27.8, 40.7, 53.1, 57.4, 63.8 and 70.6 ° attesting for the formation of a bayerite phase ($Al(OH)_3$) when Al_2O_3 was submitted to a thermal treatment in water in agreement with earlier reports [14-16], although the experimental conditions used in the present work differed substantially from those of these earlier studies. The XRD pattern of the dried Ag/Al_2O_3-OH sample (not shown) was found to be identical to that of the parent Al_2O_3-OH shown in Fig. 3. After calcination of Ag/Al_2O_3-OH at 550 °C, the XRD pattern closely resembled that of the parent Al_2O_3 support suggesting that the bayerite phase likely mainly transformed into η-Al_2O_3 [20-2122], since the XRD patterns of γ-Al_2O_3 and η-Al_2O_3 differ only little from each other [20-22], and probably also transformed back to γ-Al_2O_3 to a limited extent [20,22].

Similar UV-visible spectra were obtained for calcined Ag/Al_2O_3 and Ag/Al_2O_3-OH (Fig. 4). Three bands were observed at 210, 240 and 350 nm on both samples. Whereas the band at 210 nm has been attributed to Ag^+ [9,23], the attribution of those at 240 and 350 nm are still the subject of controversy. The band at 240 nm has been assigned to the presence of Ag^+ [23] and partially charged Ag clusters ($Ag_n^{\delta+}$) [9], whereas that at 350 nm has been attributed to the presence of partially charged Ag clusters ($Ag_n^{\delta+}$) [24] as well as that of small metallic clusters (Ag_n) [9]. Note that the silver plasmon characteristic of Ag metal particles is usually located above 390 nm [23]. From these UV-visible results and the fact that Ag coordination numbers determined earlier by EXAFS were found to remain extremely low under various experimental conditions including those of H_2-HC-SCR [25], it can be assumed that Ag is mainly present in an oxidized state in both samples.

As shown earlier, the characterization of Ag/Al_2O_3 samples by NO_x-TPD provided unique information about the coverage of Al_2O_3 by Ag which could not be obtained by other means [6,8]. The NO_x-TPD profiles obtained for the hydroxylated samples are shown in Fig. 5a. For comparison, those obtained earlier [6] on Al_2O_3 and Ag/Al_2O_3 are displayed in Fig. 5b. Whereas it can be clearly seen that the introduction of Ag on Al_2O_3 led to both a significant decrease in the NO_x uptake (446 µmol NO_x/g for Al_2O_3 compared to 337 µmol NO_x/g_{Al2O3} for Ag/Al_2O_3) and a shift of the low temperature desorption peak to higher temperatures (Fig. 5b), this was not observed for the hydroxylated samples. Fig. 5a shows that the NO_x profiles of Ag/Al_2O_3-OH and Al_2O_3-OH are similar in shape, albeit slightly different from those found on Al_2O_3 (Fig. 5b). In addition the NO_x uptakes determined on the hydroxylated samples were found to be similar for Al_2O_3-OH (439 µmol NO_x/g) and Ag/Al_2O_3-OH (442 µmol NO_x/g_{Al2O3}) and fairly close to that of Al_2O_3 (446 µmol NO_x/g). Since the transformation of the bayerite domains likely leads to the formation of η-Al_2O_3 [20-22], we found of interest to perform an additional NO_x-TPD experiment on a η-Al_2O_3 support

(SASOL, 314 m^2/g) to compare the NO_x adsorption capacity of η-Al_2O_3 to that of γ-Al_2O_3. The NO_x-TPD profile obtained for η-Al_2O_3 (not shown) was found to be similar in shape to that obtained earlier on γ-Al_2O_3 [6], but of higher intensity (761 μmol NO_x/g compared to 446 μmol NO_x/g for γ-Al_2O_3). Taking into account the specific surface areas of 314 m^2/g for η-Al_2O_3 and 180 m^2/g for γ-Al_2O_3, the amounts of NO_x adsorbed normalized per unit surface area (NO_x surface density) are found to be very close on both polymorphs (2.4 and 2.5 μmol NO_x/m^2 on η- and γ-alumina, respectively). Zecchina and co-workers [28] also found that the total amounts of NO_x adsorbed from NO_2 on γ- and δ- Al_2O_3 correlated with the specific surface areas of both polymorphs, indicating, in other words, that the NO_x surface density of alumina was unaffected by the nature of its polymorph.

4. Discussion

The treatment of the pristine Al_2O_3 support in water at 80 °C for 24 h prior to Ag deposition led to a drastic improvement of the low-temperature H_2-C_3H_6-SCR (Ag/Al_2O_3-OH) performance compared to the Ag/Al_2O_3 sample prepared on the as-received Al_2O_3 support (Fig. 2a). In contrast, the C_3H_6-SCR performance was found to be comparable on both samples and was thus found not to be influenced to a significant extent by a prior thermal treatment in water of the alumina support (Fig. 1a).

XRD characterization showed that the thermal pretreatment in water led to the hydroxylation of Al_2O_3 with the appearance of reflections attributed to the formation of a bayerite phase ($Al(OH)_3$, Fig. 3). The fact that the XRD patterns of Al_2O_3-OH and Ag/Al_2O_3-OH in their calcined state closely resembled those of γ-Al_2O_3 and Ag/γ-Al_2O_3 indicates that the bayerite phase likely transformed to η-Al_2O_3 and γ-Al_2O_3 after calcination at 550 °C. The extent of transformation of the bayerite domains to η-Al_2O_3 and γ-Al_2O_3 could not be quantified as the η-Al_2O_3 and γ-Al_2O_3 XRD patterns are only subtlety different from each

other [20-22] and that complete conversion of γ-Al_2O_3 to bayerite did not occur (Fig. 3). The UV-visible characterization of calcined Al_2O_3-OH and Ag/Al_2O_3-OH indicated that their Ag speciation was comparable (Fig. 4). Much more interesting is the characterization of the various samples by NO_x-TPD. We reported earlier [6] that the addition of Ag to Al_2O_3 led to a decrease in the NO_x uptake (Fig. 5b) and concluded that Ag occupied some of the Al_2O_3 sites responsible for NO_x adsorption (Scheme 1, Path A). It must be recalled that the NO_x adsorption sites of partly dehydroxylated Al_2O_3 samples have been attributed to Al^{3+} [26,27], O^{2-} [27,28] and OH [27] groups. In the case of the samples prepared from hydroxylated Al_2O_3, the situation is clearly different as the NO_x uptakes of Al_2O_3-OH and Ag/Al_2O_3-OH remained close to that found on Al_2O_3 (Fig. 5a and section 3.2.). The higher NO_x uptake of Ag/Al_2O_3-OH compared to that of Ag/Al_2O_3 (Fig. 5a) cannot be attributed to the likely presence of η-Al_2O_3 domains issued from the transformation of the bayerite ones since it was found that the specific surface area of both samples did not change significantly (section 2.3.) and that the NO_x surface density of η-Al_2O_3 and γ-Al_2O_3 was similar (end of section 3.2.). For Ag/Al_2O_3-OH, it can therefore be concluded that Ag anchored essentially onto sites newly-created by the thermal pretreatment of γ-Al_2O_3 in water, which were not available on the untreated support as illustrated in Scheme 1 (Path B), thus leaving the sites present initially on γ-Al_2O_3 accessible to the adsorption of NO_x. This newly-created sites most likely belong to the bayerite domains formed by thermal pretreatment in water of γ-Al_2O_3 as indicated by XRD (Fig. 3).

In a recent investigation, we showed that H_2-C_3H_6-SCR performance unexpectedly decreased as the Ag surface density (Ag/nm^2_{Al2O3}) increased [8]. The H_2-C_3H_6-SCR kinetic study highlighted the importance of the NO_x coverage in this reaction, based on structure-activity (NO_x uptake-kinetic parameters) correlations. In particular, the increase in the NO reaction order from 0 for C_3H_6-SCR to 0.4 for H_2-C_3H_6-SCR on Ag(0.7 Ag/nm^2_{Al2O3})/Al_2O_3

was assigned to a depletion in the coverage of NO_x adsorbed species due to a drastic increase in the H_2-C_3H_6-SCR reaction rate compared to that of C_3H_6-SCR [8]. Likewise, the decrease in H_2-C_3H_6-SCR catalytic performance observed as the Ag surface density increased was attributed to a decrease in the NO_x coverage due to the anchoring of Ag species onto Al_2O_3 sites also responsible for NO_x adsorption, in agreement with the observed decrease in NO_x uptake [8]. As indicated by the NO_x-TPD characterization of the samples studied in the present work (Fig. 5), the NO_x uptake found on Ag/Al_2O_3-OH remained close to that of Al_2O_3 and Al_2O_3-OH but much larger than that of Ag/Al_2O_3. This suggests that NO_x coverage on Ag/Al_2O_3-OH would be higher than that on Ag/Al_2O_3 despite the fact that their surface areas were found to be similar for both samples (section 2.3.). The higher NO_x coverage on Ag/Al_2O_3-OH compared with Ag/Al_2O_3 could thus account for the much higher H_2-C_3H_6-SCR performance found on Ag/Al_2O_3-OH compared to Ag/Al_2O_3 (Fig. 2a). In the absence of H_2 in the reacting feed, the similar C_3H_6-SCR performance found on both Ag samples (Fig. 1a) is consistent with the absence of NO partial pressure dependency (0^{th} reaction order with respect to NO for C_3H_6-SCR [8]) and thus with the absence of NO_x coverage dependency for the C_3H_6-SCR reaction. The close C_3H_6-SCR performance obtained on Ag/Al_2O_3-OH and Ag/Al_2O_3 (Fig. 1a) is also consistent with the fact that the Ag speciation on both samples was found to be similar as indicated by UV-visible characterization (Fig. 4).

Although it is widely acknowledged in the community that the starting supporting oxide/oxyhydroxide is of the utmost importance for the Ag/Al_2O_3 system, studies in which the SCR performance of Ag/Al_2O_3 was compared within samples synthesized under identical conditions from various supporting oxide/oxyhydroxides (Al_2O_3, AlOOH, $Al(OH)_3$) are rare. To our knowledge, only two studies have been reported to date in which the influence of the starting support was investigated [13,29]. Although calcination of the oxyhydroxides supports eventually leads to Al_2O_3, from here on the samples studied in these earlier works will be

denoted as Ag/starting oxide/oxyhydroxides for the sake of clarity. Zhang and Kaliaguine reported that Ag/AlOOH exhibited the best C_3H_6-SCR performance compared to Ag/Al_2O_3 and $Ag/Al(OH)_3$ [13]. Regarding $Ag/Al(OH)_3$, (i) its very low surface area, leading to a silver density (3.1 Ag/nm^2_{Al2O3}) well above the optimum Ag density highlighted recently (0.7 Ag/nm^2_{Al2O3}, [6]) and (ii) the presence of a significant amount of carbonates prevented a fair comparison of its C_3H_6-SCR performance with that of the two other samples. In contrast Ag/Al_2O_3 and Ag/AlOOH exhibited comparable specific surface areas (~ 140 m^2/g) and thus we could calculate that their Ag surface densities were similar and close to 0.8 Ag/nm^2_{Al2O3}. The higher C_3H_6-SCR performance of Ag/AlOOH compared to that of Ag/Al_2O_3 was attributed by Zhang and Kaliaguine to the higher dispersion of Ag on AlOOH due to the greater concentration of OH groups in AlOOH compared to Al_2O_3 [13]. In addition, Zhang and Kaliaguine showed that Ag was present in a more oxidized state on Ag/AlOOH than on Ag/Al_2O_3 [13]. It must be recalled here that oxidized Ag species have been reported to be the active sites of HC-SCR promoted or not by H_2 [1,7,9,24-31]. As indicated by the UV-visible data of the present study (Fig. 4), Ag speciation was found to be comparable for our Ag/Al_2O_3-OH and Ag/Al_2O_3 samples suggesting similar dispersion, so that it is not surprising that both catalysts eventually exhibited close C_3H_6-SCR performance (Fig. 1a).

In a recent study, He and co-workers reported on the superiority of Ag/AlOOH compared to Ag/Al_2O_3 and $Ag/Al(OH)_3$ in C_2H_5OH-SCR after calcination of the samples at 600 °C [29]. These authors suggested that the C_2H_5OH-SCR activity was correlated to the amount of tetrahedrally-coordinated Al^{3+} cations supposed to be the active sites of the adsorption and activation of the –NCO intermediates [29]. Toops and co-workers initially proposed that atomic hydrogen may be formed on the surface of a Ag/Al_2O_3 catalyst under a C_2H_5OH-SCR feed via the dissociative adsorption of ethanol [32]. The presence of molecular H_2 has been recently detected in the course of methanol-assisted HC-SCR [33] and methanol-

SCR [34,35] reactions. This led these authors [33-35] to the proposal that the high SCR performance found at low-temperature in the presence of alcohols was due, at least partly, to a similar effect as that of H_2 in H_2-HC-SCR [8]. According to the results of the present study, in which it is proposed that the higher H_2-C_3H_6-SCR performance of Ag/Al_2O_3-OH compared to Ag/Al_2O_3 would be attributed to the higher NO_x coverage on Ag/Al_2O_3-OH due to the preferential interaction of Ag with newly created OH groups, the higher C_2H_5OH-SCR performance of Ag/AlOOH compared to Ag/Al_2O_3 reported in [29] could be accounted for by a similar reason. Ag anchoring on AlOOH sites different from those of Al_2O_3 would help preserve a higher NO_x density in the final catalyst as shown in the present work. This explanation, however, cannot stand as the only reason to describe the order of C_2H_5OH-SCR activity found by He and co-workers [29]: Ag/AlOOH > Ag/Al_2O_3 > $Ag/Al(OH)_3$. $Ag/Al(OH)_3$ was found to exhibit the lowest C_2H_5OH-SCR performance among the samples investigated indeed, whereas it could have been expected that this particular catalyst should have provided a catalytic performance at least higher than that of Ag/Al_2O_3 on the sole basis of the conclusions drawn in our present work. As highlighted above, the C_2H_5OH-SCR reaction must behave closer to H_2-HC-SCR than to HC-SCR [33-35] and we have reported recently that the performance of Ag/Al_2O_3 catalysts increased as the Ag loading, i.e. Ag surface density, decreased in H_2-C_3H_6-SCR [8]. This is consistent with the fact that Ag/Al_2O_3 samples with Ag contents lower than 2 wt% were found to be more active in C_2H_5OH-SCR than the Ag(2 wt%)/Al_2O_3 sample [36,37]; Ag(2 wt%)/Al_2O_3 has been reported to be the optimum catalyst in HC-SCR [6] but not in H_2-HC-SCR [8] indeed. In the work of He and co-workers, the surface areas of Ag/AlOOH (213.1 m^2/g), Ag/Al_2O_3 (197.9 m^2/g) and $Ag/Al(OH)_3$ (168.1 m^2/g) were found to be substantially different after calcination at 600 °C [29]. The order of activity reported for these catalysts in C_2H_5OH-SCR (Ag/AlOOH > Ag/Al_2O_3 > $Ag/Al(OH)_3$) also follows the order expected from the calculated Ag surface

densities of the corresponding samples (Ag/AlOOH : 0.5 Ag/nm^2_{Al2O3} < Ag/Al_2O_3 : 0.6 Ag/nm^2_{Al2O3} < $Ag/Al(OH)_3$: 0.7 Ag/nm^2_{Al2O3}). To summarize, in addition to the potential involvement of tetrahedrally-coordinated Al^{3+} cations in C_2H_5OH-SCR [29], the superiority of the Ag/AlOOH catalyst compared to Ag/Al_2O_3 and $Ag/Al(OH)_3$ in C_2H_5OH-SCR reported in [29] may also result from differences in the NO_x coverage on the corresponding samples influenced by (i) the preferential interaction of Ag with AlOOH anchoring sites different from those found on Al_2O_3, as highlighted in the present work, and/or (ii) the Ag surface density of the samples [8].

5. Conclusion

This work highlights for the first time that a thermal treatment in water of γ-Al_2O_3 prior to Ag deposition leads to a drastic enhancement of H_2-C_3H_6-SCR performance at low temperature. Based on an earlier H_2-C_3H_6-SCR kinetic investigation [8] and on the NO_x uptake data, this improvement is attributed to the higher NO_x coverage on Ag/Al_2O_3-OH compared with Ag/Al_2O_3. The higher NO_x adsorption capacity of Ag/Al_2O_3 prepared from the γ-Al_2O_3 support thermally-pretreated in water is proposed to result from the preferential interaction of Ag with newly-created Al_2O_3 anchoring sites ($Al(OH)_3$ bayerite domains), which were not available on the untreated pristine support. The identification of the latter sites is currently being investigated. The present work may also provide arguments on the fact that boehmite (AlOOH) is known to be a preferred starting Al_2O_3 precursor for the preparation of Ag/Al_2O_3 catalysts in the HC-SCR field, as however scarcely discussed in the corresponding literature.

Acknowledgments

Dr. T. Chaieb gratefully acknowledges UPMC for financial support (PhD Grant 322/2012). The authors also thank Prof. X. Carrier for providing the η-Al_2O_3 (SASOL) support and Dr. S. Boujday for fruitful discussions.

Figure Captions

Fig. 1. (a) Conversion of NO_x to N_2 (solid lines) and selectivity to N_2 (dashed lines), and (b) conversion of C_3H_6 to CO_x in the C_3H_6-SCR reaction on Ag/Al_2O_3 (grey) and Ag/Al_2O_3-OH (black). For comparison, the data obtained previously on a different batch of Ag/Al_2O_3 sample [6] are also reported (●,○). 0.18 g of Ag/Al_2O_3 in 0.18 g of Al_2O_3. Feed composition: 385 ppm NO_x, 400 ppm C_3H_6, 8% O_2 and He balance with a 230 mL_{NTP}/min flow rate.

Fig. 2. (a) Conversion of NO_x to N_2 (solid lines) and selectivity to N_2 (dashed lines), and (b) conversions of C_3H_6 to CO_x (solid lines), and H_2 (dotted lines) in the H_2-C_3H_6-SCR reaction on Ag/Al_2O_3 (grey) and Ag/Al_2O_3-OH (black). For comparison, the data obtained previously on a different batch of Ag/Al_2O_3 sample [8] are also reported (●,○). 0.18 g of Ag/Al_2O_3 in 0.18 g of Al_2O_3. Feed composition: 0.21 % H_2, 385 ppm NO_x, 400 ppm C_3H_6, 8% O_2 and He balance with a 230 mL_{NTP}/min flow rate.

Fig. 3. XRD patterns of Al_2O_3 calcined for 2 h at 550 °C, Al_2O_3-OH dried at 120 °C for 12 h and Ag/Al_2O_3-OH dried at 120 °C for 12 h and calcined for 2 h at 550 °C. Al_2O_3 (JCPDS 79-1558), Bayerite (JCPDS 20-11).

Fig. 4. UV-vis spectra of Ag/Al_2O_3-OH (black) and Ag/Al_2O_3 (grey) after calcination at 550 °C for 2 h.

Fig. 5. NO_x-TPD profiles on (a) Al_2O_3-OH (-○-) and Ag/Al_2O_3-OH and (b) Al_2O_3 (-○-) and Ag/Al_2O_3 [6] after exposure of 0.18 g of sample to 385 ppm NO_x and 8% O_2 in He (230 mL_{NTP}/min flow rate) at RT for about 4 h.

Scheme 1. Simplified representation of the influence of the hydroxylation process of Al_2O_3 on the deposition of Ag species (●), and the distribution of the NO_x species adsorbed on thermally-treated (Δ) Al_2O_3 surfaces starting from the as-received Al_2O_3 (path (A)) and Al_2O_3-OH (path (B)).

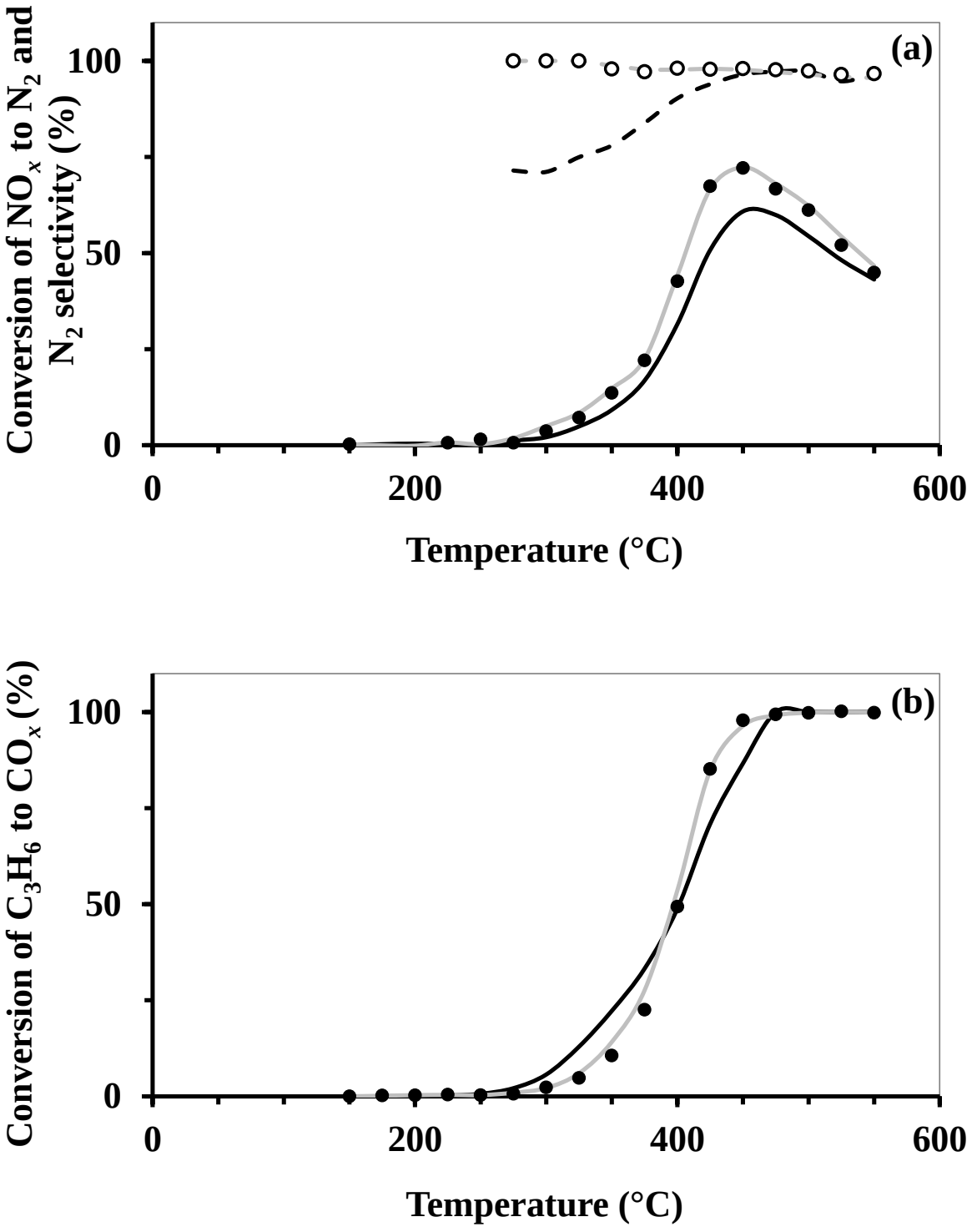
(a)
Conversion of NO_x to N_2 and N_2 selectivity (%)
100
50
0
0
200
400
600
Temperature (°C)
(b)
Conversion of C_3H_6 to CO_x (%)
100
50
0
0
200
400
600
Temperature (°C)

Fig. 1

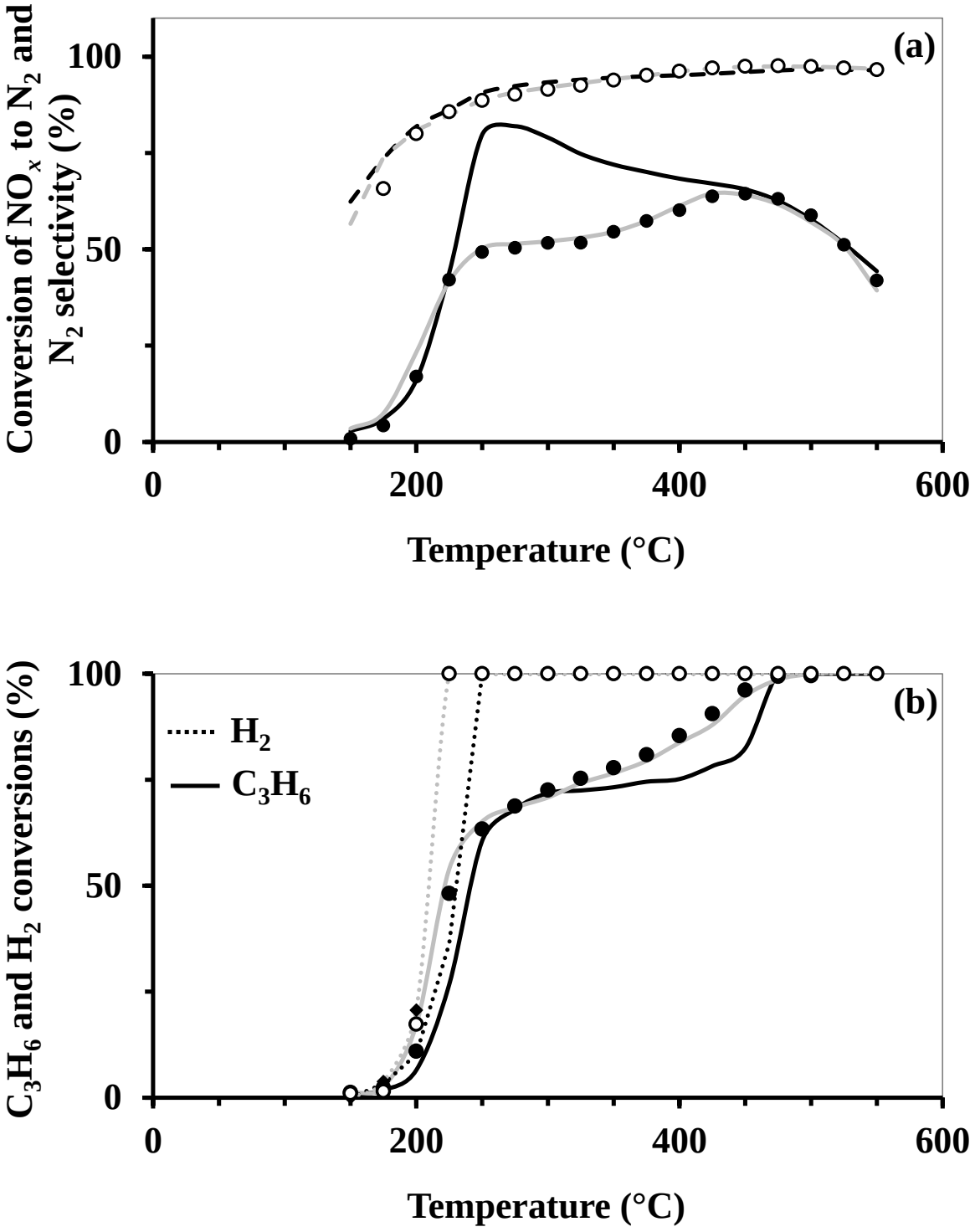
(a)
Conversion of NO_x to N_2 and N_2 selectivity (%)
100
50
0
0
200
400
600
Temperature (°C)
(b)
H_2
C_3H_6
C_3H_6 and H_2 conversions (%)
100
50
0
0
200
400
600
Temperature (°C)

Fig. 2

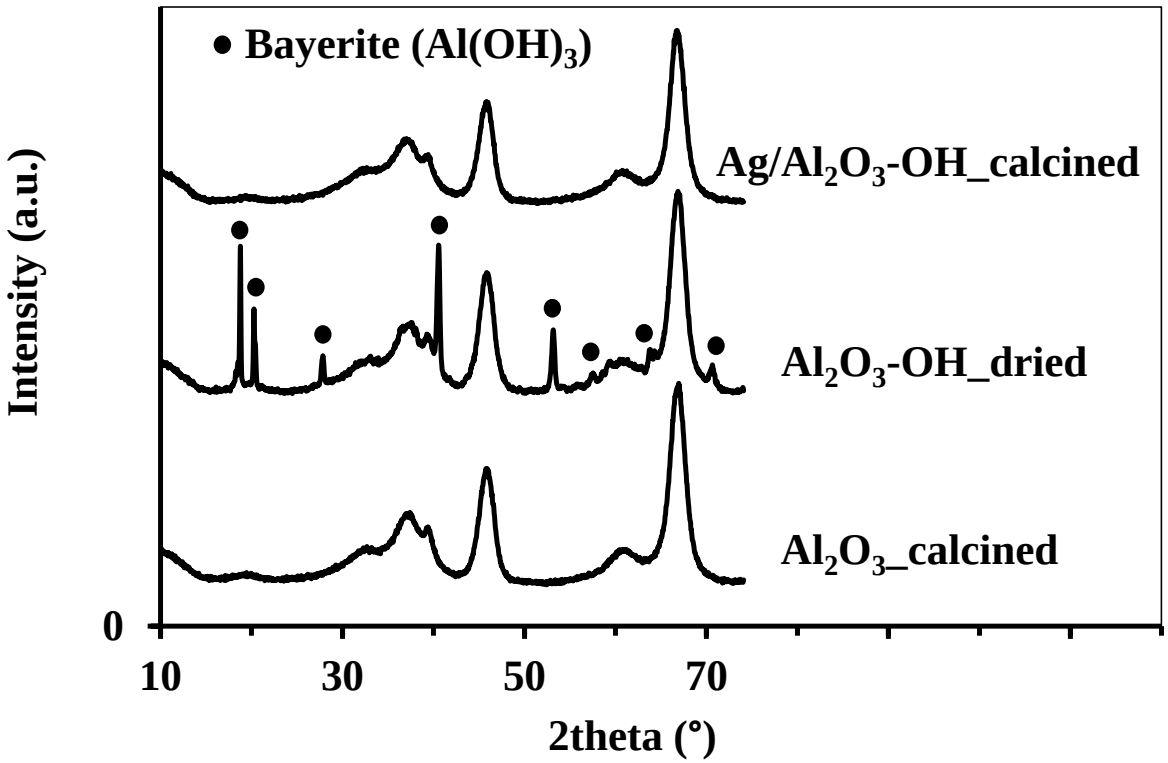
● Bayerite (Al(OH)3)
Ag/Al2O3-OH_calcined
Al2O3-OH_dried
Al2O3_calcined
Intensity (a.u.)
0
10
30
50
70
2theta (°)

Fig. 3

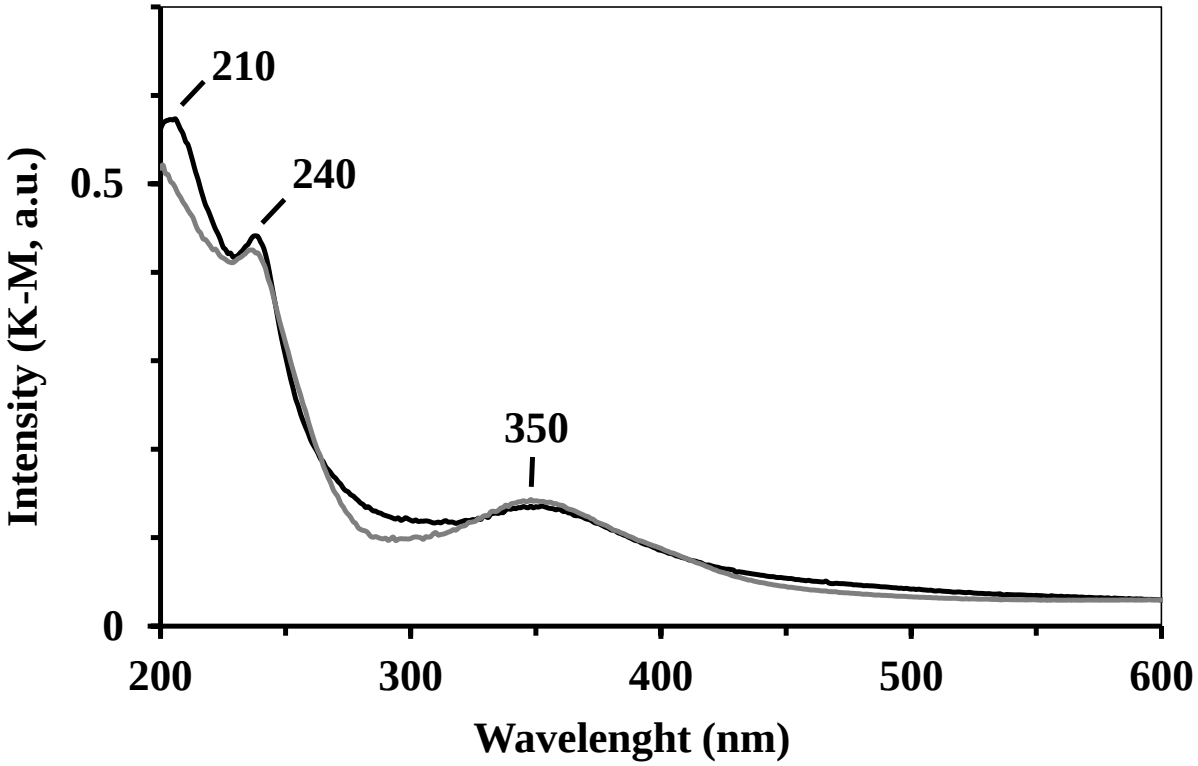
210
240
350
0.5
0
Intensity (K-M, a.u.)
200
300
400
500
600
Wavelenght (nm)

Fig. 4

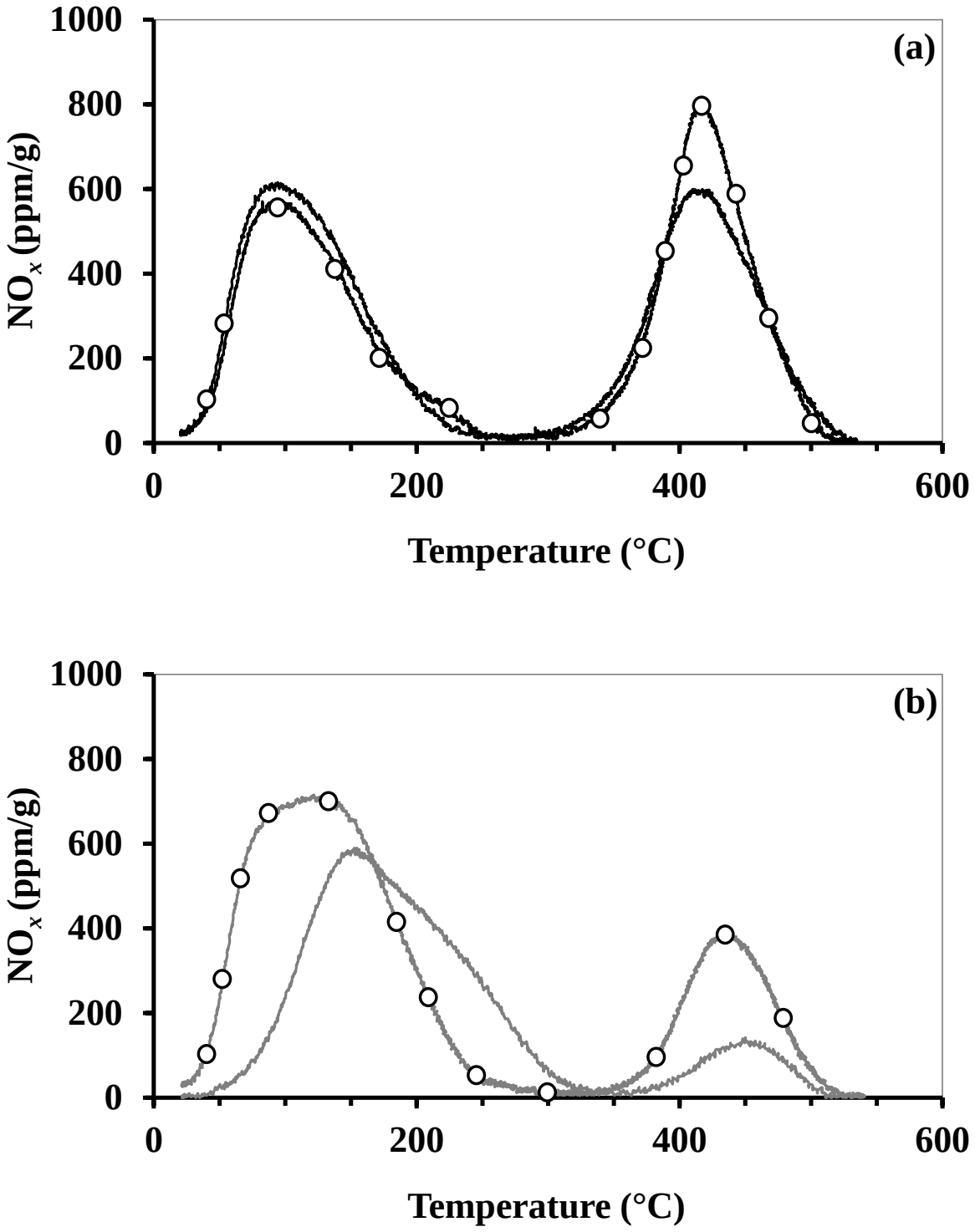
(a)
1000
800
600
400
200
0
NOx (ppm/g)
0
200
400
600
Temperature (°C)
(b)
1000
800
600
400
200
0
NOx (ppm/g)
0
200
400
600
Temperature (°C)

Fig. 5

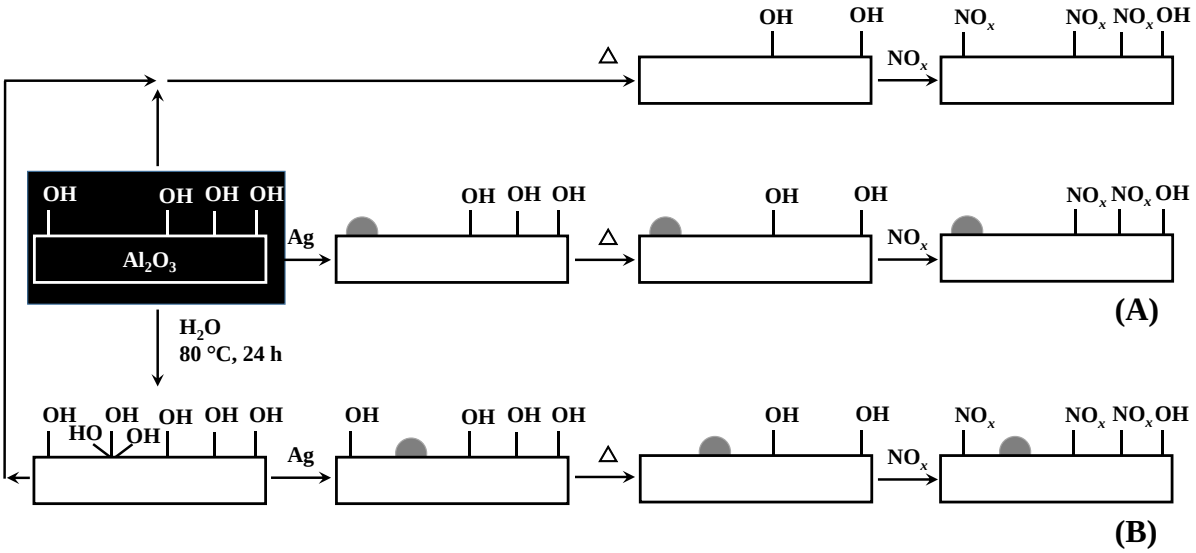
OH
OH
NOx
NOx NOx OH
Δ
OH OH OH OH
Al2O3
Ag
OH OH OH
OH
OH
NOx NOx OH
(A)
H2O
80 °C, 24 h
OH OH OH OH OH
HO
OH
Ag
OH
OH OH OH
OH
OH
NOx
NOx NOx OH
(B)

Scheme 1.

References

[1] Burch R (2004) Catal. Rev. Sci. Eng. 46:271.

[2] Epling B, Peden C, Nova I (2014) Catal. Today 231:1.

[3] Miyadera T (1993) Appl. Catal. B 2:199.

[4] Satokawa S (2000) Chem. Lett. 29:294.

[5] Satokawa S, Shibata J, Shimizu K-I, Satsuma A, Hattori T (2003) Appl. Catal. B: Environnemental 42:179.

[6] Chaieb T, Delannoy L, Louis C, Thomas C (2013) Appl. Catal. B: Environmental 142-143:780.

[7] Liu F, Yu Y, He H (2014) Chem. Commun. 50:8445.

[8] Chaieb T, Delannoy L, Costentin G, Louis C, Casale S, Chantry RL, Li ZY, Thomas C (2014) Appl. Catal. B: Environmental 156-157:192.

[9] Kamolphop U, Taylor SFR, Breen JP, Burch R, Delgado JJ, Chansai S, Hardacre C, Hengrasmee S, James SL (2011) ACS Catal. 1:1257.

[10] Petitto C,Delahay G (2012) Catal. Lett. 142:433.

[11] Ralphs K, D'Agostino C, Burch R, Chansai S, Gladden LF, Hardacre C, James SL, Mitchell J, Taylor SFR (2014) Catal. Sci. Technol. 4:531.

[12] Ralphs K, Chansai S, Hardacre C, Burch R, Taylor SFR, James SL (2015) Catal. Today 246:198.

[13] Zhang R, Kaliaguine S (2008) Appl. Catal. B: Environmental 78:275.

[14] Franck JP, Freund E, Quéméré E (1984) J. Chem. Soc. Chem. Commun. 10:341.

[15] Lefèvre G, Duc M, Lepeut P, Caplain R, Fédoroff M (2002) Langmuir 18:7530.

[16] Carrier X, Marceau E, Lambert J-F, Che M (2007) J. Colloid Interface Sci. 308:429.

[17] Mironenko RM, Belskaya OB, Talsi VP, Gulyaeva TI, Kazakov MO, Nizovskii AI, Kalinkin AV, Bukhtiyarov VI, Lavrenov AV, Likholobov VA (2014) Appl. Catal. A: General 469:472.

[18] Law HY, Blanchard J, Carrier X, Thomas C (2010) J. Phys. Chem. C 114:9731.

[19] Thomas C (2011) J. Phys. Chem. C 115:2253.

[20] Zhou R-S, Snyder RL (1991) Acta Cryst. 47:617.

[21] Pecharromán C, Sobrados I, Iglesias JE, González-Carreño T, Sanz J (1999) J. Phys. Chem. B 103:6160.

[22] Busca G (2013) Catal. Today 226:2.

[23] Bogdanchikova N, Meunier FC, Avalos-Borja M, Breen JP, Pestryakov A (2002) Appl. Catal. B 36:287.

[24] She X, Flytzani-Stephanopoulos M (2006) J. Catal. 237:79.

[25] Breen JP, Burch R, Hardacre C, Hill CJ (2005) J. Phys. Chem. B 109:4805.

[26] Venkov T, Hadjiivanov K, Klissurski D (2002) Phys. Chem. Chem. Phys. 4:2443.

[27] Szanyi J, Kwak JH, Chimentao RJ, Peden CHF (2007) J. Phys. Chem. C 111:2661.

[28] Pazé C, Gubitosa G, Orso Giacone S, Spoto G, Llabrés i Xamena FX, Zecchina A (2004) Topics Catal. 30/31:169.

[29] Deng H, Yu Y, He H (2015) J. Phys. Chem. C 119:3132.

[30] Sazama P, Čapek L, Drobná H, Sobalík Z, Dědeček J, Arve K, Wichterlová B (2005) J. Catal. 232:302.

[31] Kim PS, Kim MK, Cho BK, Nam I-S, Oh SH (2013) J. Catal. 301:65.

[32] Johnson II WL, Fisher GB, Toops TJ (2012) Catal. Today 184:166.

[33] Chansai S, Burch R, Hardacre C, Norton D, Bao X, Lewis L (2014) Appl. Catal. B: Environmental 160-161:356.

[34] Männikkö M, Skoglundh M, Härelind H (2015) Catal. Today 258:454.

[35] Männikkö M, Wang X, Skoglundh M, Härelind H (2016) Appl. Catal. B: Environmental 180:291.

[36] Kyriienko P, Popovytch N, Soloviev S, Orlyk S, Dzwigaj S (2013) Appl. Catal. B: Environmental 140-141:691.

[37] Deng H, Yu Y, Liu F, Ma J, Zhang Y, He H (2014) ACS Catal. 4:2776.